Bull. Disas. Prev. Res. Inst., Kyoto Univ., Vol. 36, Parts 3, 4, No. 321, December, 1986

Stability of Slender Reinforced Concrete Columns Subjected to Biaxially Eccentric Loads

By Satoshi IWAI, Koichi MINAMI and Minoru WAKABAYASHI

(Manuscript received October 11, 1986)

Abstract

The elastic-plastic behavior of pin-ended reinforced concrete slender columns subjected to biaxially eccentric loads is investigated experimentally and theoretically. The ultimate loads, longitudinal and transverse deformations and the behavior up to failure of the columns are examined in detail.

A total of 36 column specimens with rectangular cross sections including square sections were tested. The ratios of column length to minimum depth ranged from 6 to 26. Loads were applied monotonically at each column end with equal eccentricities at various angles from an axis of symmetry. The ultimate load carrying capacity of a slender column is reduced by additional eccentricity due to lateral deflection even in a column having a length to depth ratio of 15. The numerical analysis to solve the load-deformation response of the column predicts the test behavior very well. In the case of square columns, there is not much difference in the ultimate loads of the columns in spite of variation of the angle of eccentricity of the applied load. However, the remarkable effects of biaxial bending on the elastic-plastic behavior occurs with the rectangular columns. When the rectangular columns are subjected to biaxially eccentric load to cause bending about the near-strong axis, the ultimate loads and the deformation behavior are significantly affected by the bending about the weak axis of the section.

1. Introduction

Columns in building are designed conventionally on the basis of a structural analysis of frames in the planes in which the principal axes of columns are constructed. However, since almost all columns are subjected to biaxial bending, the effects of biaxial bending on the behavior of columns should be investigated. A number of experiments and analyses have been done to investigate the ultimate strength of short reinforced concrete columns under biaxially eccentric loading, and many strength formulations have been proposed for their design.

Investigations on instability problems of relatively slender concrete columns have been extensively carried out in the area of no fear of strong earthquakes, while the shear resistance of short columns has been more investigated in Japan. In AIJ Standard[1], slender reinforced concrete columns are regulated by the following limitations of Art. 15.7;

> The ratio of the minimum depth or diameter of a member to the distance between the main supporting points shall be not less than 1/15 and 1/10 in case of using ordinary concrete and light weight concrete, respectively. These limitations, however, are not applied when the structural safety of the column is certified by struc-

tural calculation considering the effective slenderness ratio.

In recent years, as the material strengths of concrete and steel increase more and more, the cross sections are able to be designed to compact and the members become to be slender. Moreover the reinforced concrete braces with slender proportions are sometimes used in a frame to resist earthquake forces. Therefore, clarification of the elastic-plastic behavior of slender reinforced concrete columns is very important.

The column behavior under biaxial loading becomes further complex due to the slenderness effects. There is very little available experimental information of the stability of slender columns. In this paper, fundamental data from biaxially eccentric loading tests of slender columns with square and rectagular cross sections[2),3)] are reported. The objective of this study is to investigate the slenderness effects under biaxial bending on the ultimate strength and the deformation behavior up to the failure of reinforced concrete columns.

2. Outline of Experimental Work

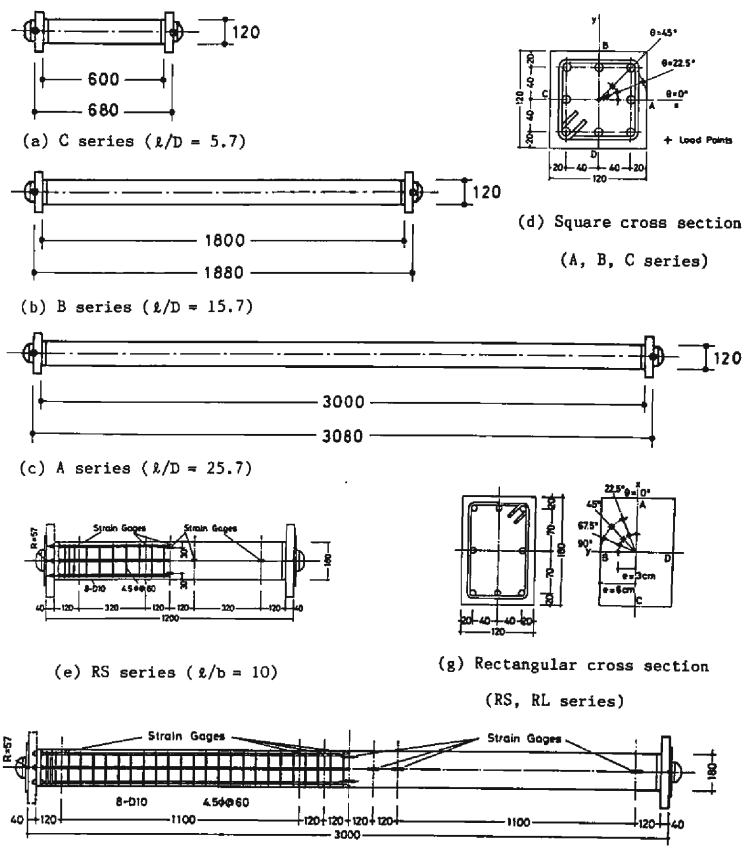

Fig. 1 Geometry of test specimen (units in mm).

Table 1 Mix proportion of concrete and material properties (unit: 1 t/cm² = 0.098 kN/mm²).

Test Series	C	B	A	R
Mixing Ratios by Weight				
Water	0.67	0.65	0.66	0.62
Cement	1	1	1	1
Sand	1.97	1.91	1.91	1.90
Gravel	2.74	2.76	2.76	2.75
Specific Gravities				
Cement	3.16	3.16	3.16	3.16
Sand	2.61	2.62	2.45	2.48
Gravel	2.58	2.60	2.50	2.54
Concrete				
Compressive Strength F_c (kg/cm²)	275	281	311	316
Strain at Compressive Strength ε_p (10^{-3})	2.59	2.30	2.41	2.43
Splitting Tensile Strength (kg/cm²)	—	30.1	26.2	28.9
Reinforcement				
Upper Yield Strength (t/cm²)	3.72	3.72	3.63	3.77
Lower Yield Strength (t/cm²)	3.54	3.62	3.49	3.68
Ultimate Strength (t/cm²)	5.27	5.17	5.50	5.18
Elongation (10^{-2})	18.2	16.9	22.6	27.2

A total of 36 column specimens were tested. Their column length to minimum section depth rations, l/D or l/b, ranged from 6 to 26. The geometry of test specimens is shown in **Fig. 1.** The columns had a 12 cm(b) × 12 cm(D) square cross section or a 12 cm(b) × 18 cm(D) rectangular cross section with 8-D10 longitudinal bars (gross reinforcement ratios of 0.0396 and 0.0264, respectively) and 4.5 mm hoops spaced 6 cm apart. The mix proportion of concrete and the properties of materials are listed in **Table** 1. The concrete was cast in the horizontal position using a machined metal-form. The compressive strength of the concrete was 270-340 kgf/cm² (26-33 N/mm²) and the tensile yield strength of main reinforcement was 3,500-3,700 kgf/cm² (340-360 N/mm²). Age of specimens at test was 40-210 days.

Photo 1 and **Fig. 2(a)** show a specimen placed in the loading apparatus. Both ends of the column were supported by universal bearings to simulate pin-ended conditions. The bearings were greased to minimize friction. Load was applied monotonically at each column end with equal eccentricities, e, at various angles, θ, from an axis of symmetry, as given in **Fig. 1.** Transverse deflections, u and v in the principal axes of the section, denoted by x and y, respectively, and torsional rotation, α, at the mid-height of the column (**Fig. 2(b)**), rotations of both column ends, θ_x and θ_y (where added subscripts, u and l, represented upper end and lower end, respectively), about the x and y axes of the section, respectively, and axial deformation, w,

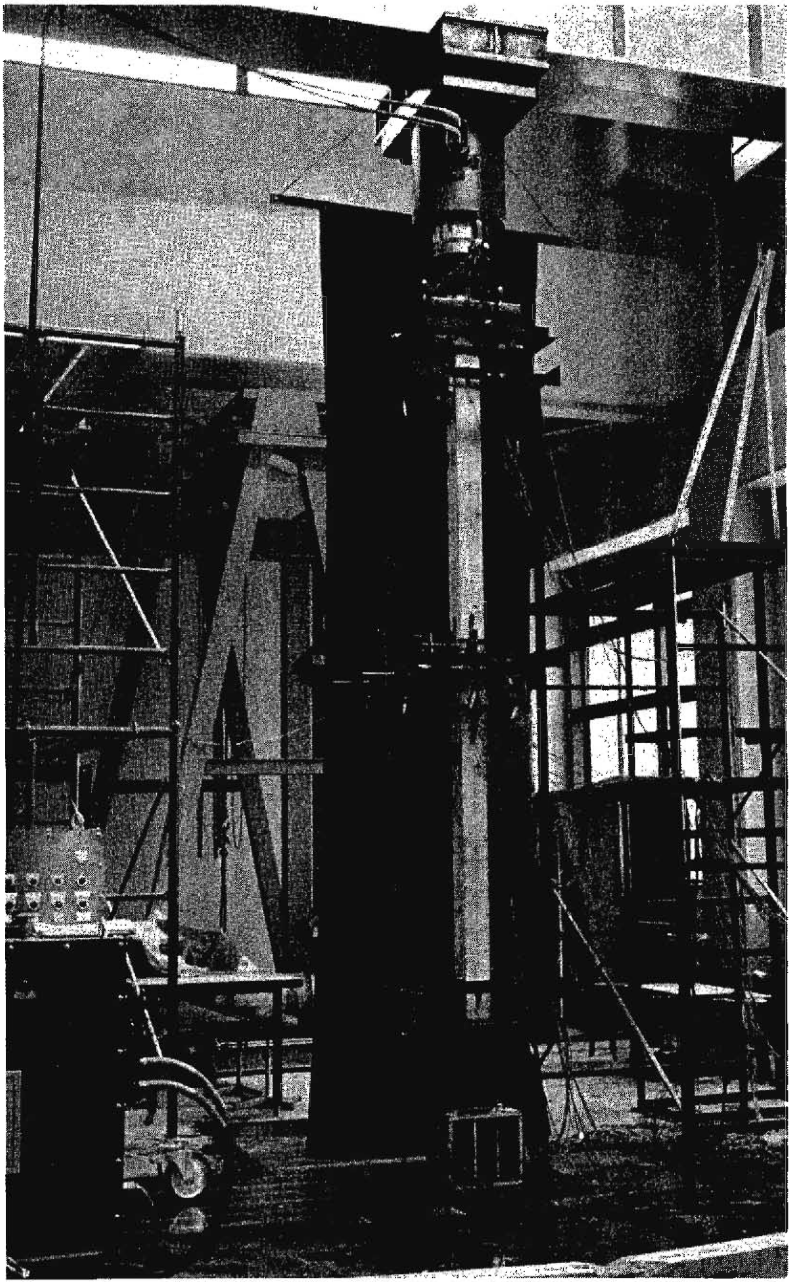

Photo. 1 Overall view of test of A000b.

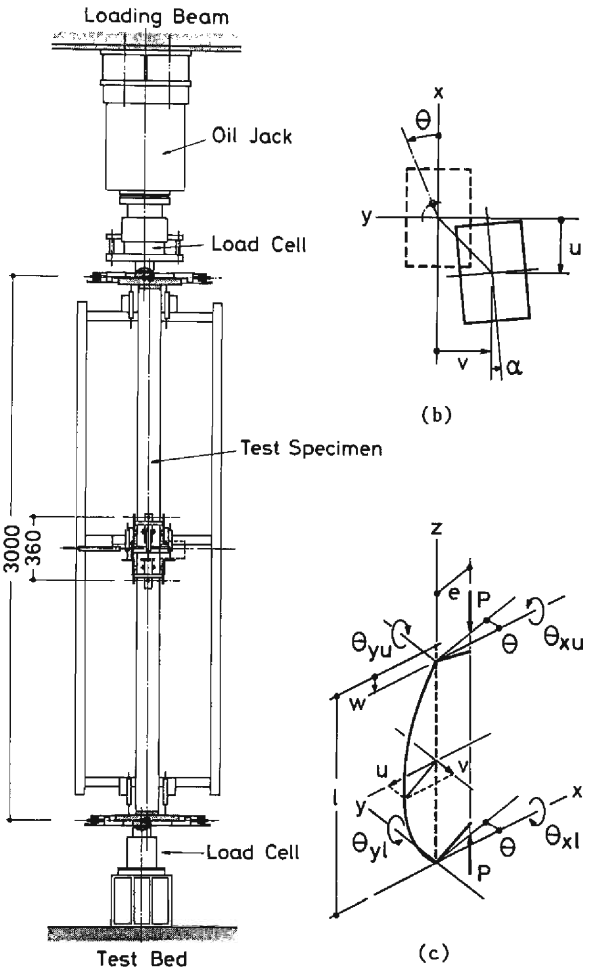

Fig. 2 Specimen in loading apparatus (units in mm).

(**Fig. 2(c)**) were measured by potentio-meters. Those potentio-meters were supported on a rigid frame running parallel to the line of action of the applied load. Typical arrangements of the instrumentation devices are shown in **Fig. 3**. Load was measured by load cells installed at the ends of the columns. The strains on concrete surface and in reinforcing bars were measured by potentio-meters and strain gages at some selected locations.

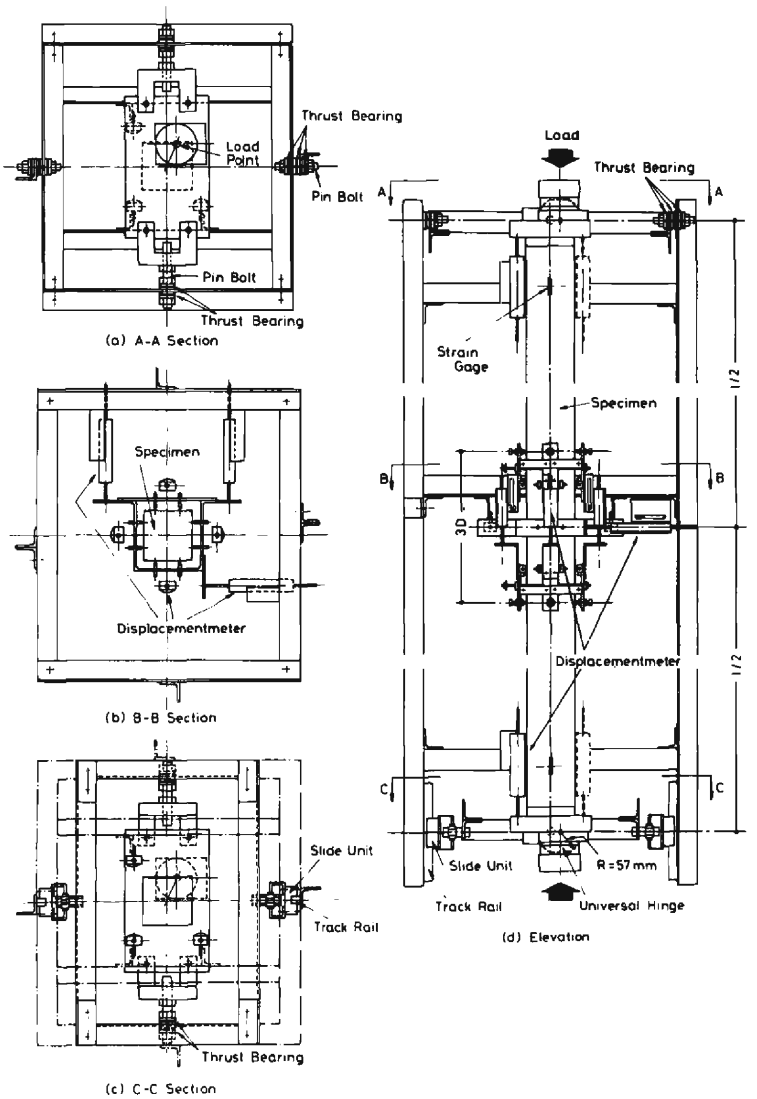

Fig. 3 Measuring device of long column.

3. Method of Theoretical Analysis

The load-deformation response of the column was solved by the numerical method of a second-order analysis[4] taking into account the effects of deflections and changes in stiffness of the columns on moments and forces. The following basic assumptions have been made:

(1) lateral deflections of the column are small compared to its length and the curvatures are represented by the second derivatives of the deflections;

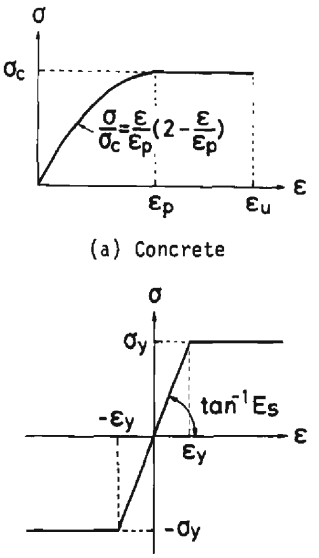

Fig. 4 Assumption of stress-strain relationships.

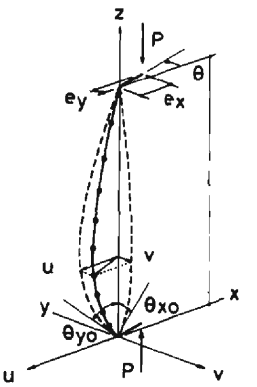

Fig. 5 Notation relating to column analysis.

(2) plane sections remain plane after deformation;

(3) effects of shear on lateral deflection and rotation of the cross section due to torsional deformation are negligible;

(4) the assumed stress-strain relationships for the concrete and the reinforcing bars are shown in **Fig. 4(a)** and **4(b)**, respectively. Strain reversal is not considered. The concrete is unable to sustain any tensile stress.

The effect of the strain reversal on the analytical results is discussed later.

A symmetrically reinforced rectangular cross section is considered and an x-y axis system is taken with the origin at the centroid of the section (**Fig. 1**). A force P is assumed to act at the point which is defined in the x-y axis by the eccentricities e_x and e_y, as shown in **Fig. 5**. If the assumptions of perfect bonding and plane distribution of strains are made, the strain, ε, in the section can be defined by the three quantities ε_0, ϕ_x and ϕ_y.

$$\varepsilon=\varepsilon_0+x\cdot\phi_y+y\cdot\phi_x \quad \cdots\cdots (1)$$

in which ε_0=strain at the centroid and ϕ_x, ϕ_y=curvatures produced by bending moment components, M_x and M_y, about the x and y axes, and are positive when they cause compression in the positive y and x directions, respectively. Knowing the strain distribution, the axial force, N, and the bending moments, M_x and M_y, are calculated from the assumed stress-strain relationships. In the present study, the concrete and the reinforcing bars are partitioned into many small elemental areas. The total force and the moments in the section are then evaluated by summation of the

elemental forces acting on the elemental areas and the moments of the elemental forces, respectively.

A pin ended reinforced concrete column shown in **Fig. 5** is considered for the case of monotonic loads P applied with biaxial eccentricities at each end. The lateral deflections, u and v, of the column are assumed to be small, so that the curvatures ϕ_x and ϕ_y can be expressed in the form of second derivatives of deflections

$$\phi_x = -\frac{d^2v}{dz^2} \quad \cdots\cdots (2a)$$

$$\phi_y = -\frac{d^2u}{dz^2} \quad \cdots\cdots (2b)$$

For the given load $P=N$, the deflections u and v also have to satisfy conditions of external equilibrium, namely

$$M_x(\phi_x, \phi_y) = P(v+e_y) \quad \cdots\cdots (3a)$$

$$M_y(\phi_x, \phi_y) = P(u+e_x) \quad \cdots\cdots (3b)$$

The equilibrium shape can be determined by the solution of simultaneous equations for the various unknowns P, u, v, M_x, M_y, ϕ_x and ϕ_y, using equations (2) and (3). Using the first derivatives of deflections about the x and y axes, θ_x and θ_y, the curvatures are given by

$$\phi_x = -\frac{d\theta_x}{dz} \quad \cdots\cdots (4a)$$

$$\phi_y = -\frac{d\theta_y}{dz} \quad \cdots\cdots (4b)$$

Therefore the second-order simultaneous differential equations (2) and (3) can be replaced by the first-order simultaneous equations expressed as

$$\frac{du}{dz} = \theta_y \quad \cdots\cdots (5a)$$

$$\frac{dv}{dz} = \theta_x \quad \cdots\cdots (5b)$$

$$M_x\left(-\frac{d\theta_x}{dz}, \ -\frac{d\theta_y}{dz}\right) = P(v+e_y) \quad \cdots\cdots (5c)$$

$$M_y\left(-\frac{d\theta_x}{dz}, \ -\frac{d\theta_y}{dz}\right) = P(u+e_x) \quad \cdots\cdots (5d)$$

The column length l is divided into several segments of the same length. For equations (5), application of the Runge-Kutta-Gill numerical integration method and the Newton-Raphson iteration technique yields the deflections u and v corresponding to the load, P. In this numerical analysis, the column length was divided into 10 segments, and the square and the rectangular cross sections were divided into 10×10 and 10×15 elements, respectively. As the condition of convergence of calculation, deviation of deflection at the end of a column was limited to less than 1/10,000 of the column length. Convergence for the given load level was achieved within two or

three applications of the Newton-Raphson technique.

4. Test Results Compared with Analytical Results

The test results are summarized in **Table 2.**

Figure 6 shows the experimental strain distributions across the section for several load levels for square short columns C 000, C 020 and C 210. The concrete strains and the reinforcing bar strains may be seen to conform closely to the plane strain distribution. It is only near maximum load level that there occurs some deviation from the plane strain distribution. The strain in concrete just before crushing was 0.004–0.005 for the columns subjected to biaxially eccentric loads. Final collapse was

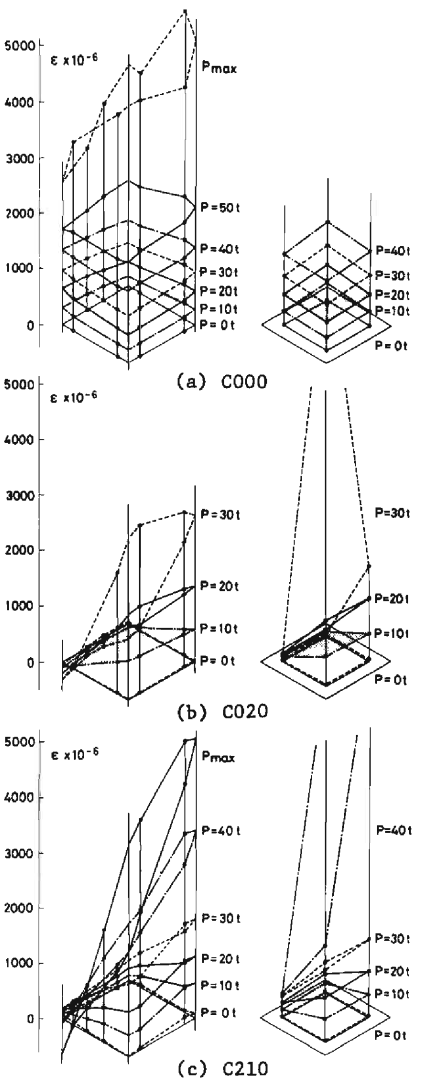

Fig. 6 Strain distributions across the section at increasing load levels; concrete strain (left) and steel strain (right).
(a) Concentric loading.
(b) Uniaxial loading.
(c) Biaxial loading.

Table 2 Summary of test results (unit: 1 t=9.8 kN).

l	Specimen	θ	e	$P=P_{max}$										
cm	name	deg	cm	P_{max} t	u mm	v mm	w mm	α deg	θ_{xu} deg	θ_{yu} deg	θ_{xl} deg	θ_{yl} deg	$p\varepsilon_{max}$ $\times10^{-3}$	$g\varepsilon_{max}$ $\times10^{-3}$
Square columns														
	C000	0	0	57.1									4.04	5.64
	C205	22.5	0.6	51.4									4.16	5.23
	C210	22.5	1.2	43.3									4.23	5.15
68.0	C220	22.5	2.4	30.0									4.75	4.71
	C250	22.5	6.0	18.0									5.41	—
	C020	0	2.4	33.4									4.64	6.98
	C420	45	2.4	33.3									5.01	6.42
	B000	0	0	47.9	5.09	−0.18	3.40	0.01	0.00	0.50	0.03	0.51	2.56	2.73
	B205	22.5	0.6	46.2	2.46	4.45	3.03	−0.02	0.43	0.43	0.51	0.39	2.71	2.88
	B210a	22.5	1.2	35.8	7.73	6.45	2.41	−0.02	0.64	0.83	0.67	0.84	3.13	3.13
188.0	B210b	22.5	1.2	34.4	9.76	6.76	2.65	−0.01	0.73	0.99	0.73	1.00	3.97	4.80
	B220	22.5	2.4	25.4	14.09	9.19	1.80	−0.01	0.92	1.46	0.97	1.49	4.62	3.84
	B250	22.5	6.0	13.4	20.45	11.13	0.56	−0.02	1.21	2.32	1.18	2.28	4.34	4.36
	B020	0	2.4	27.7	14.09	−0.82	1.66	−0.03	−0.09	1.52	−0.09	1.49	2.96	3.39
	B420	45	2.4	23.2	11.78	14.64	1.72	−0.02	1.55	1.20	1.52	1.18	5.08	3.83
	A000a	0	0	55.4	5.2	4.4	5.87	−0.04	0.06	0.08	0.21	0.16	3.32	2.89
	A000b	0	0	54.9	5.8	5.4	—	—	—	—	—	—	—	—
	A205	22.5	0.6	32.6	12.1	14.6	3.42	−0.07	0.93	0.74	0.89	0.85	2.59	2.98
308.0	A210	22.5	1.2	28.0	13.5	10.9	2.50	−0.02	0.65	0.78	0.71	0.90	2.13	2.41
	A220	22.5	2.4	18.9	25.7	17.4	2.19	0.07	1.06	1.58	1.05	1.59	2.87	2.57
	A250	22.5	6.0	10.9	42.3	22.5	1.65	−0.07	1.45	2.73	1.48	2.79	3.23	3.39
	A020	0	2.4	18.8	33.7	−1.2	2.16	−0.07	−0.12	2.00	−0.04	2.06	2.24	2.41
	A420	45	2.4	17.2	20.6	25.4	2.08	−0.04	1.52	1.26	1.54	1.24	2.75	2.73
Rectangular columns														
	RS300	0	3.0	61.4	3.77	0.49	1.76	0.01	0.07	0.60	0.13	0.65	3.54	4.38
	RS322	22.5	3.0	59.1	3.23	4.28	1.67	−0.02	0.74	0.59	0.81	0.62	4.14	4.48
120.0	RS345	45.0	3.0	50.0	2.11	6.00	0.97	−0.04	1.26	0.36	1.08	0.40	4.12	4.42
	RS367	67.5	3.0	43.4	0.58	8.36	1.45	−0.01	1.54	0.17	1.46	0.09	4.22	5.25
	RS390	90.0	3.0	42.8	−0.18	8.78	1.56	−0.02	1.43	−0.13	1.54	−0.08	4.44	4.18
	RL300	0	3.0	48.4	20.57	1.50	3.88	0.02	−0.02	1.30	0.18	1.36	2.70	3.13
	RL322	22.5	3.0	35.5	10.29	19.57	2.64	−0.06	1.31	0.68	1.35	0.75	2.54	3.15
	RL345	45.0	3.0	28.4	6.08	27.49	2.14	−0.05	1.64	0.39	1.74	0.45	2.32	2.94
300.0	RL367	67.5	3.0	24.1	2.46	29.32	1.66	0.02	1.78	0.21	1.83	0.22	1.97	2.27
	RL390	90.0	3.0	23.5	0.40	39.42	1.83	0.01	2.37	−0.03	2.47	0.02	2.19	3.12
	RL622	22.5	6.0	18.7	15.16	26.94	1.49	0.03	1.65	1.00	1.71	1.04	2.79	2.97
	RL645	45.0	6.0	14.5	8.73	36.78	1.23	−0.07	2.43	0.64	2.48	0.68	2.33	2.86
	RL667	67.5	6.0	12.5	2.92	43.59	0.95	−0.07	3.04	0.22	3.10	0.33	2.34	2.93

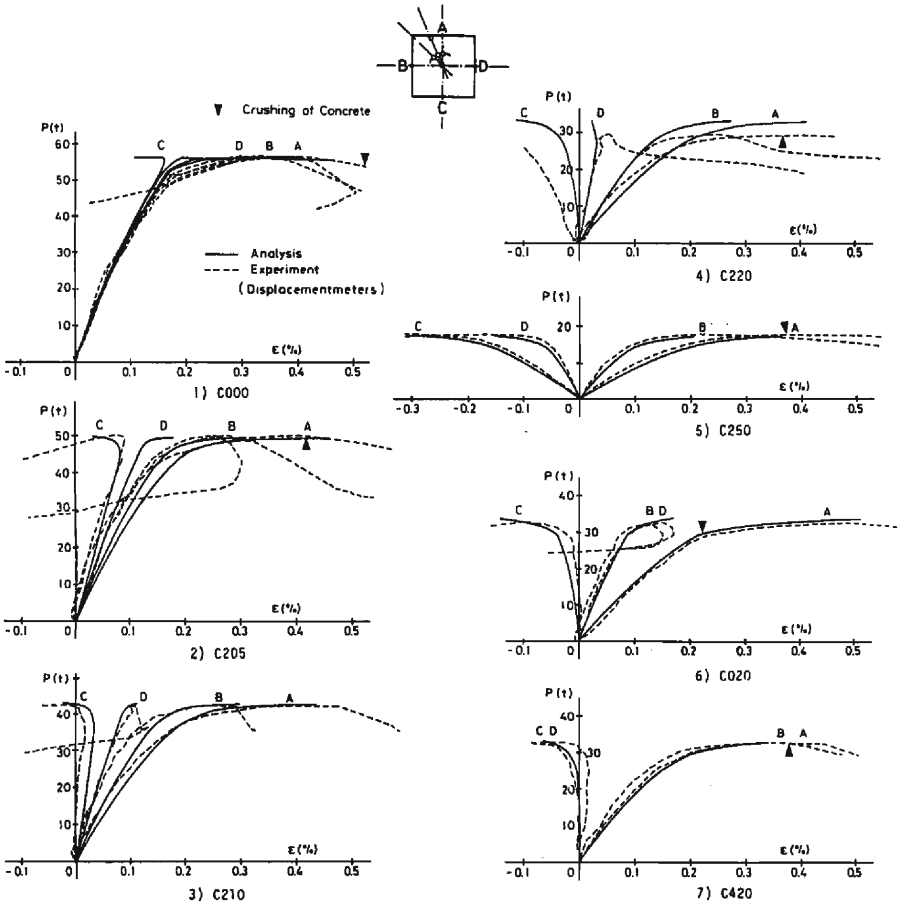

Fig. 7 Load versus longitudinal strain relationships (C series) (unit: 1 t=9.8 kN).

accompanied by spalling of concrete in the compression zone. This immediately resulted in the buckling of longitudinal reinforcement between ties at the compression corner. All columns except one case, specimen C 220, deflected symmetrically with respect to the column mid-height and failed at the mid-height section. In **Fig. 7**, the test results of load-strain relationships obtained from the longitudinal strain data at the selected positions (A, B, C and D) of the mid-height section are compared with the analytical results. The broken lines and the solid lines denote the test data and the analytical data, respectively. By this analytical method, the test behavior of load and strain of the short columns is seen to be well predicted.

Figures 8 and **9** show the load-deflection curves and the load-strain curves, respectively, for the square long columns of $l/D=25.7$. The solid lines and the broken lines in **Fig. 8** indicate deflections at mid-height, u and v, respectively. The thin lines correspond to the test results and the thick line to the analytical results. In the test, crushing of concrete occured at the descending branch after the peak load.

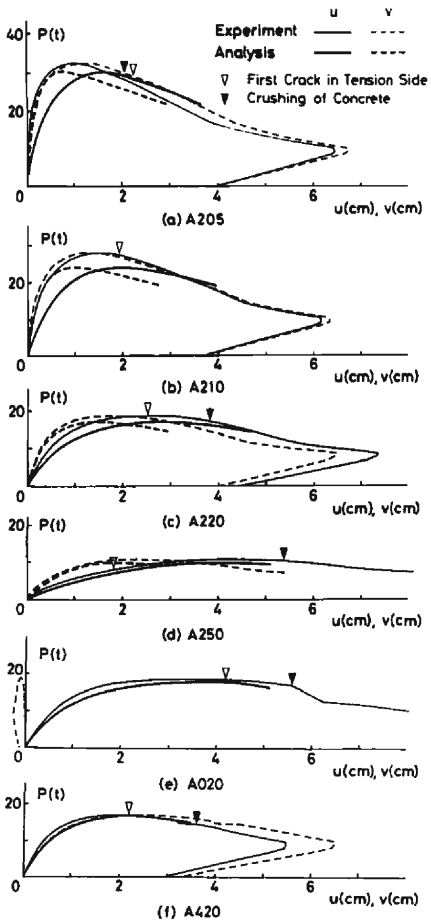

Fig. 8 Load-deflection relationships (A series) (unit: 1 t=9.8 kN).

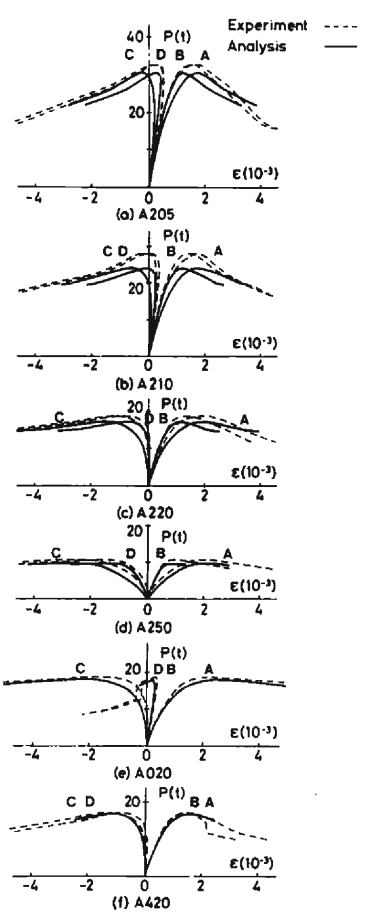

Fig. 9 Load versus longitudinal strain relationships (A series) (unit: 1 t=9.8 kN).

The load decreased suddenly just after the crushing of concrete and the column was failed. The numerical analysis adopted herein need not take the strain reversal into consideration. The reason for this can be seen in the following. The experimental strains at the compression and tension zone increase monotonically with increasing load in each zone and strain reversal occurs in only a range of small strain near the neutral axis of the section, as shown in **Figs. 7** and **9**. Therefore it is regarded that the ultimate strength and the deformation behavior of the columns are scarcely affected by the strain reversal.

Figure 10 shows the change of mid-height deflections with increasing load. In the case of square columns under biaxial loading at the angle of $\theta=22.5°$ (**Fig. 10** (a)), the direction of deflection corresponds closely to the plane including the load-

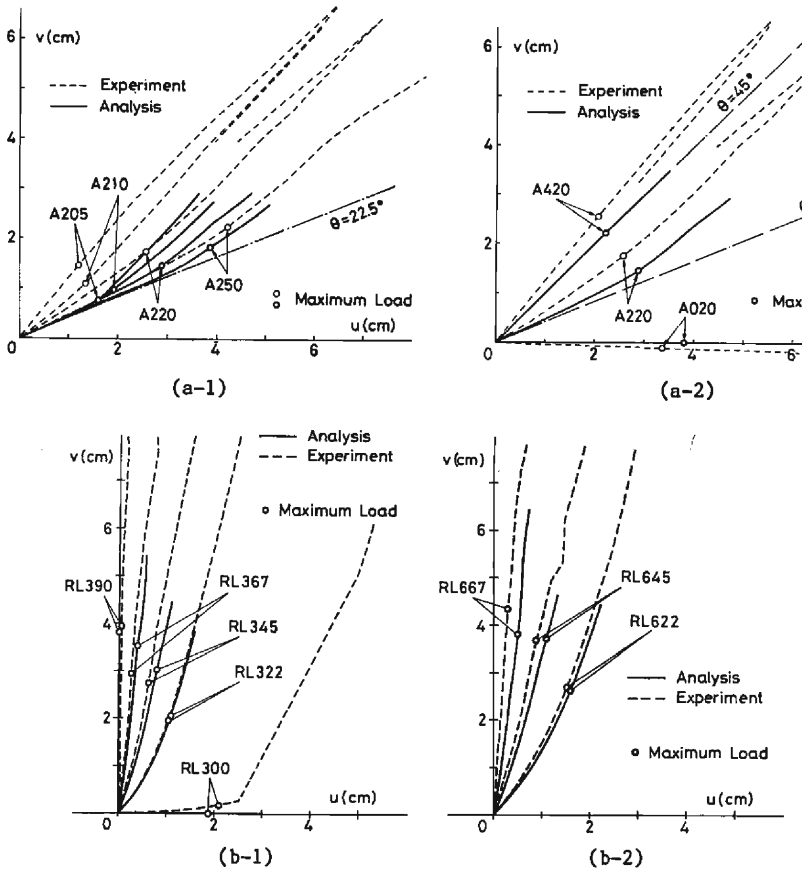

Fig. 10 Change of mid-height deflections with increasing load.
(a-1, a-2) A series.
(b-1, b-2) RL series.

ing points and the centroids of the end section, before reaching the maximum load. However, after the attainment of the maximum load, the column has a tendency to deflect away from that plane. In the case of rectangular columns (**Fig. 10(b)**), the lateral deflections significantly depend on bending about the weak axis of the section. The numerical analysis to solve the load-deformation response of the column is seen to predict the test behavior very well. The torsional deformation α in biaxially eccentric loads was very small, as shown in **Table 2**, and the effect is negligible. The maximum torsional angle was measured to be only 0.6°. From these test results, it is confirmed that the assumption of no torsional deformation is useful to the analysis.

5. Ultimate Loads of Biaxially Loaded Short Columns

The ratios of the maximum load by the test to that by the numerical analysis, P_{test}/P_{cal}, for every square short columns are listed in **Table 3** and displayed by bars in **Fig. 11**. Analytical results agree well with the test results. In the same figure, predicted values obtained by Bresler's method[5] and Ramamurthy's method[6] are represented. Bresler and Ramamurthy proposed expressions for the shape of the interaction surface for a reinforced concrete column section with biaxial bending from

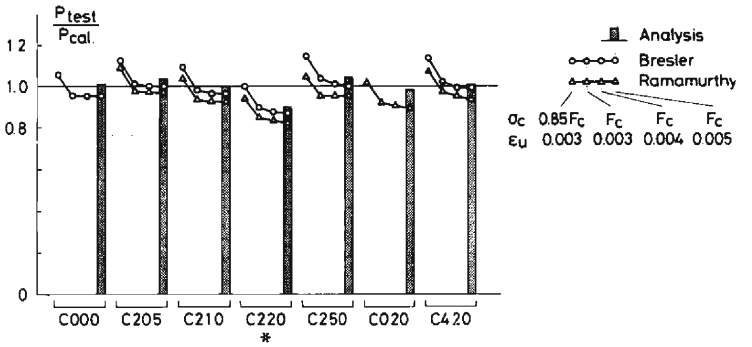

Fig. 11 Comparison of ultimate loads of short columns (C series).
*: failed at column end.

Table 3 Summary of analytical results of square short columns (unit: 1 t=9.8 kN).

Specimen	P_{test}	P_{cal}(t) (P_{test}/P_{cal})								
			$\sigma_c=0.85F_c$		$\sigma_c=F_c$					
Name	(t)	Analysis	$\varepsilon_u=0.003$		$\varepsilon_u=0.003$		$\varepsilon_u=0.004$		$\varepsilon_u=0.005$	
			I *	II*	I	II	I	II	I	II
C000	57.1	56.5 (1.011)	53.9 (1.059)	53.9 (1.059)	59.8 (0.955)	59.8 (0.955)	59.8 (0.955)	59.8 (0.955)	59.8 (0.955)	59.8 (0.955)
C205	51.4	49.6 (1.036)	45.7 (1.125)	47.2 (1.089)	50.8 (1.012)	52.6 (0.977)	51.3 (1.002)	52.9 (0.972)	51.4 (1.000)	53.0 (0.970)
C210	43.3	43.3 (1.000)	39.6 (1.093)	41.6 (1.041)	44.1 (0.982)	46.3 (0.935)	44.8 (0.967)	46.7 (0.927)	44.8 (0.967)	46.7 (0.927)
C220	30.0	33.3 (0.901)	30.0 (1.000)	31.9 (0.940)	33.4 (0.898)	35.4 (0.847)	34.2 (0.877)	36.0 (0.833)	34.5 (0.870)	36.6 (0.820)
C250	18.0	17.2 (1.047)	15.7 (1.146)	17.2 (1.047)	17.3 (1.040)	18.9 (0.952)	17.8 (1.011)	18.9 (0.952)	18.0 (1.000)	18.9 (0.952)
C020	33.4	33.9 (0.985)	32.7 (1.021)	32.7 (1.021)	36.3 (0.920)	36.3 (0.920)	36.9 (0.905)	36.9 (0.905)	37.4 (0.893)	37.4 (0.893)
C420	33.3	33.0 (1.009)	29.3 (1.137)	31.0 (1.074)	32.6 (1.021)	34.3 (0.971)	33.5 (0.994)	35.0 (0.951)	33.5 (0.994)	35.6 (0.935)

* I: Bresler's Method
II: Ramamurthy's Method

which, knowing the uniaxial strengths, the biaxial bending strengths may be calculated.

An expression derived by Bresler[5] for the strength of a biaxially loaded column is

$$\frac{1}{P_u}=\frac{1}{P_x}+\frac{1}{P_y}-\frac{1}{P_0} \quad \cdots\cdots (6)$$

where P_u=ultimate load under biaxial bending, P_x=ultimate load under uniaxial bending when only eccentricity e_x is present, P_y=ultimate load under uniaxial bending when only eccentricity e_y is present, and P_0=ultimate load when there is no eccentricity. Values of P_x and P_y are obtained from the interaction functions that represent the section capacity under uniaxial loading conditions.

Ramamurthy[6] proposed two equations to define approximately the shape of M_x-M_y interaction curves in square and rectangular columns with eight or more bars, equally distributed among the faces. The locus of the ultimate radial moment M_u at any load level in square columns is approximately defined by

$$M_u=M_{uy0}\{1-0.1\,(\theta/45°)\} \quad \cdots\cdots (7)$$

where M_{uy0}=ultimate uniaxial moment about y axis corresponding to load P under consideration and $\theta(\text{deg.})=\tan^{-1}(e_y/e_x)$=inclination of the line joining the load point to the centroid of the section to x axis. Equation (7) yields $M_u=0.9\,M_{uy0}$ for $\theta=45°$. M_u for any value of θ is calculated by linear interpolation between bending about a major principal axis and bending about a diagonal.

Using the rectangular stress block with a constant ultimate stress σ_c and a failure limit strain ε_u to represent concrete in the analysis of cross section strength[7], interaction curves under uniaxial loading conditions were calculated in four cases; (1) $\sigma_c=0.85\,F_c$ (F_c=compressive strength of cylinder) and $\varepsilon_u=0.3\%$, (2) $\sigma_c=F_c$ and $\varepsilon_u=0.3\%$, (3) $\sigma_c=F_c$ and $\varepsilon_u=0.4\%$, and (4) $\sigma_c=F_c$ and $\varepsilon_u=0.5\%$.

The majority of calculated values obtained from Bresler's method were less than those obtained from Ramamurthy's method. All calculated values for the cases where $\sigma_c=F_c$ was assumed give good predictions of maximum load observed by test compared with the cases where $\sigma_c=0.85\,F_c$. However, the value of extreme fiber strain, ε_u, has slight influence on the prediction of load. The maximum load obtained by the authors' numerical analysis corresponds to the case of $\sigma_c=F_c$ and $\varepsilon_u=0.5\%$.

6. Load-Moment Behavior of Square Long Columns

The behavior of the column under increasing load is illustrated by the axial load versus bending moment diagram for the critical section of the column given in **Fig. 12**. The lateral coordinate gives the magnitude of the biaxial bending moment, M. The points for the combination of axial load and nominal end moment at the maximum strength obtained experimentally are designated by small circles for each column. The three curves denoted by "$l/D=15.7$" or "$l/D=25.7$" represent the corre-

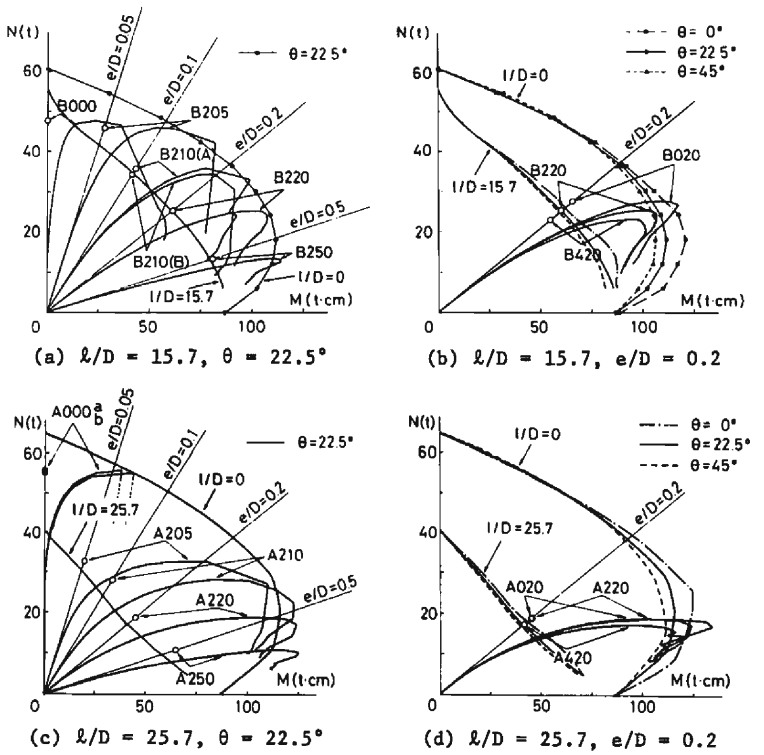

(a) $\ell/D = 15.7$, $\theta = 22.5°$ (b) $\ell/D = 15.7$, $e/D = 0.2$

(c) $\ell/D = 25.7$, $\theta = 22.5°$ (d) $\ell/D = 25.7$, $e/D = 0.2$

Fig. 12 Interaction diagrams for column section illustrating load-moment behavior up to failure (units: 1 t=9.8 kN, 1 t·cm=0.098 kN·m).

sponding analytical data. When the column is short, the additional eccentricity due to lateral deflection at the critical section is negligible and the maximum moment can be estimated by the end moment at all stages. When the N-M path with increasing load has reached the interaction line denoted by "$l/D=0$" (where $\sigma_c=F_c$ and $\varepsilon_u=2\varepsilon_p$), a material failure of the section occurs. If the column is long, the additional eccentricity at the critical section increases more rapidly at high load levels, and the N-M path is curved. The maximum load of the column eventually is reduced by the amplified bending moment caused by additional eccentricity.

There are two types of long column behavior for the case of $l/D=15.7$. When the eccentricity at the column ends is relatively large, a material failure of the section occurs causing the N-M path to reach the interaction line. However, when the load is applied with small eccentricity, the column becomes unstable before reaching the interaction line and even at the critical section the column does not demonstrate its material strength capacity. This is called an instability failure. For all columns of $l/D=25.7$, the instability failure occurred, except in the one case of $e/D=0.5$ in which material failure occurred. In the test results, the N-M path reversed to inside of the interaction line after reaching the interaction line. This is because the re-

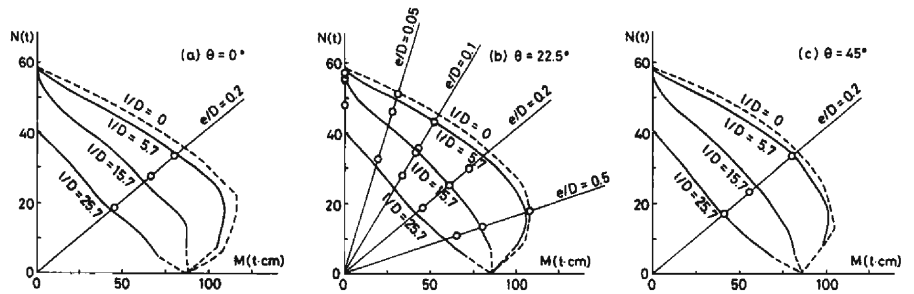

Fig. 13 Square long column interaction diagrams (units: 1 t=9.8 kN, 1 t·cm=0.098 kN·m).

Table 4 Summary of analytical results of square long columns (unit: 1 t=9.8 kN).

Specimen name	σ_c* kg/cm²	P_{max} t	u mm	v mm	θ_x deg	θ_y deg	ε_{max} $\times 10^{-3}$
B000		52.8	2.12	1.06	0.105	0.212	2.10
B205		42.1	7.42	3.39	0.350	0.773	3.11
B210		34.9	9.19	4.48	0.462	0.947	3.32
B220	280	25.4	14.30	7.64	0.777	1.49	4.37
B250		13.2	17.88	9.24	0.976	1.95	4.30
B020		26.1	13.45	0.00	0.000	1.43	2.95
B420		24.9	10.93	10.93	1.15	1.15	4.27
A000		39.1	12.1	5.0	0.30	0.72	2.05
A205		30.5	16.1	7.6	0.47	1.00	2.20
A210		24.2	19.2	9.7	0.60	1.20	2.30
A220	310	17.3	28.9	14.7	0.90	1.80	2.90
A250		9.8	38.7	18.4	1.17	2.52	3.21
A020		18.0	38.1	0.00	0.00	2.35	2.52
A420		16.9	22.0	22.0	1.38	1.38	2.92

* σ_c: Assumed concrete strength

duction of load carrying capacity of the critical section occurs by the spalling of concrete and the buckling of main reinforcements.

Figure 13 is the family of square column interaction curves giving the combination of the axial load and the end moment which cause failure of the column. Solid lines are obtained analytically, indicating the reduction in ultimate load due to slenderness for various loading cases. All the test data are plotted by the small circles. Analytical results of the maximum loads P_{max} and the deformation at $P=P_{max}$ for long columns are summarized in **Table 4**. In the case of square long columns, it is remarkable that there is not much difference of the ultimate loads of the columns in spite of variation of the angle of eccentricity of the applied load. The analytical results agree quite well with the test results.

7. Ultimate Loads of Rectangular Columns

Figure 14 shows how the maximum load P_{max} varies with changing the angle θ of eccentricity for rectangular columns subjected to uniaxially or biaxially eccentric loads. Analytical results are listed in **Table 5**. Because of the difference of load carrying capacity and bending stiffness about each of two principal axes, i.e. the strong axis and the weak axis, the maximum load of column decreases with increasing θ. For all short rectangular columns of $l=120$ cm ($l/b=10$), the material failure occured at the critical section. When the load is applied so as to cause bending about the strong axis, the effect of the additional bending moment caused by deflection on the ultimate

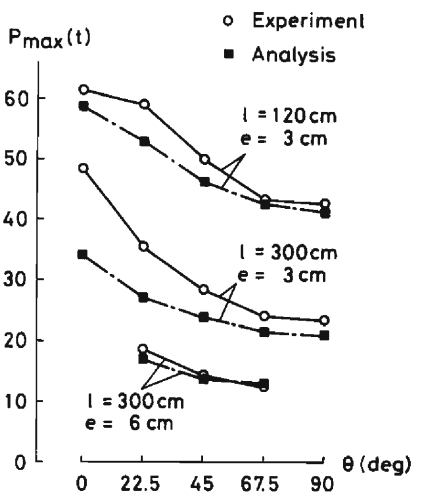

Fig. 14 P_{max}-θ relationship of rectangular columns (unit: 1 t=9.8 kN).

Table 5 Summary of analytical results of rectangular columns (unit: 1 t=9.8 kN).

Specimen name	σ_c* kg/cm²	P_{max} t	u mm	v mm	θ_x deg	θ_y deg	ε_{max} $\times 10^{-3}$
RS300		58.7	5.35	0	0	0.92	4.88
RS322		53.0	3.83	5.12	0.85	0.66	5.52
RS345	340	46.4	2.68	6.58	1.12	0.46	5.12
RS367		42.7	1.53	8.23	1.38	0.26	5.09
RS390		41.4	0	9.87	1.60	0	5.00
RL300	230	34.2	18.77	0	0	1.26	2.69
RL322	280	27.2	10.98	20.43	1.30	0.74	2.78
RL345	320	23.9	7.95	30.15	1.91	0.53	2.85
RL367	330	21.6	3.92	35.00	2.23	0.26	2.57
RL390	340	21.1	0	37.72	2.41	0	2.30
RL622	270	17.1	15.83	26.22	1.71	1.09	3.19
RL645	280	13.8	10.96	37.22	2.44	0.74	3.17
RL667	340	13.1	5.02	38.41	2.58	0.34	2.42

*σ_c : Assumed concrete strength

load is negligible. However, when the load is applied to cause bending about the near-weak axis, there is some amount of reduction of ultimate load due to the additional moment. For the long columns of $l=300$ cm ($l/b=25$), the ultimate load was affected largely by increasing deflection with increasing load and the instability failure occurred. When the columns are subjected to a biaxially eccentric load causing bending about the near-weak axis, that is, the load is applied when angle θ ranges from about 45° to 90°, the maximum load and the deformation of the columns closely resemble the behavior under uniaxially eccentric loading conditions about the weak axis. Therefore, those columns can be approximated by the columns under only uniaxial bending about the weak axis. However, when the columns are subjected to biaxially eccentric load to cause bending about the near-strong axis, with θ ranging from 0° to 45°, the ultimate strengths seriously depend on the angle of eccentricity of the applied load, as shown in **Fig. 14**, and consequently the column must be analyzed exactly by taking into account the biaxial loading effect.

8. Conclusions

The following conclusions can be drawn for the ultimate load and the deformation behavior of slender reinforced concrete columns subjected to a biaxially eccentric load.

(1) On the basis of the test results, it is recognized that the concrete and the reinforcing bar strains conform closely to the plane strain distribution even in the case of biaxial bending.

(2) The numerical analysis adopted herein to solve the load-deformation response of the column very well predicts the test behavior.

(3) The ultimate load carrying capacity of a slender column is reduced by the additional eccentricity due to lateral deflections, even in a column having a length to depth ratio of 15.

(4) In the case of square long columns, there is not much difference on ultimate loads of the columns in spite of variation of the angle of eccentricity of the applied load.

(5) In the case of rectangular long columns, when the columns are subjected to biaxially eccentric load to cause bending about the near-strong axis, the ultimate loads and the deformation behavior seriously depend on the angle of eccentricity of the applied load. Consequently those columns must be analyzed exactly by taking into account the biaxial loading effect. However, the columns subjected to biaxial bending about the near-weak axis can be approximated by that under only uniaxial bending about the weak axis.

Acknowledgment

The authors wish to express the gratitude to Dr. Takeshi Nakamura of the Disaster Prevention Research Institute, Kyoto University, for valuable discussions and critical reading of the mamuscript.

References

1) Architectural Institute of Japan: AIJ Standard for Structural Calculation of Reinforced Concrete Structures (revised 1985), Chap. 4.
2) Iwai, S.: Studies on the Elastic-Plastic Behavior of Reinforced Concrete Long Columns Subjected to Static and Dynamic Loads, Thesis submitted in partial fulfillment of the requirements for the degree of Doctor of Engineering at Kyoto University, Kyoto, Japan, Dec. 1984 (in Japanese).
3) Iwai, S., K. Minami and M. Wakabayashi: Ultimate Strength of Slender Reinforced Concrete Columns Subjected to Biaxially Eccentric Loads (Part 1 - Loading Tests of Square Cross Section Columns), Trans. Architectural Inst. of Japan, No. 367, Sep. 1986, pp. 59-68 (in Japanese).
4) Iwai, S., K. Minami and M. Wakabayashi: Ultimate Strength of Slender Reinforced Concrete Columns Subjected to Biaxially Eccentric Loads (Part 2 - Comparison of Experiment and Analysis), to be submitted to Trans. Architectural Inst. of Japan (in Japanese).
5) Bresler, B.: Design Criteria for Reinforced Columns under Axial Load and Biaxial Bending, Journal of ACI, Vol. 57, No. 5, Nov. 1960, pp. 481-490.
6) Ramamurthy, L.N.: Investigation of the Ultimate Strength of Square and Rectangular Columns under Biaxially Eccentric Loads, ACI Publication SP-13, 1966, pp. 263-298.
7) ACI Committee 318: Building Code Requirements for Reinforced Concrete (ACI 318-83), Chap. 10, 1983.

Appendix-Notation

The following symbols are used in this paper.

b = width of column section
D = depth of column section
E_s = Young's modulus of reinforcing bar
$e = \sqrt{e_x^2 + e_y^2}$, resultant eccentricity of load
e_x = component of eccentricity of load in the x direction
e_y = component of eccentricity of load in the y direction
F_c = concrete cylinder strength
l = length of column
M = biaxial bending moment
M_u = ultimate biaxial bending moment (Eq. (7))
M_{uy0} = ultimate uniaxial bending moment about the y axis (Eq. (7))
M_x = bending moment about the x axis
M_y = bending moment about the y axis
N = axial force

P=compressive load applied at the ends of column
P_{cal}=maximum load calculated by the numerical analysis
P_{max}=maximum load
P_0=ultimate load under pure axial compression (Eq. (6))
P_{test}=maximum load obtained by test
P_u=ultimate load under biaxial compression (Eq. (6))
P_x=ultimate load under compression with uniaxial eccentricity e_x (Eq. (6))
P_y=ultimate load under compression with uniaxial eccentricity e_y (Eq. (6))
u=component of lateral deflection in the x direction
v=component of lateral deflection in the y direction
w=total axial deformation of column
x=principal axis of the cross section
y=principal axis of the cross section
z=coordinate along original column axis
α=torsional rotation angle at the mid-height of column
ε=strain
ε_{max}=compression corner strain at maximum load
$_D\varepsilon_{max}$=compression corner strain at maximum load measured by potentiometers
$_G\varepsilon_{max}$=compression corner strain at maximum load measured by strain gages
ε_0=strain at the centroid of cross section
ε_p=strain at maximum stress of concrete
ε_u=failure limit strain of concrete
ε_y=yield strain of reinforcing bar
θ=inclination of plane including the loading point and the centroid of the end section to the x axis
θ_x=slope of deflection curve of column about the x axis
θ_{xl}=rotation angle of the lower end of column about the x axis
θ_{x0}=deflection slope about the x axis at origin of the z axis (see Fig. 5)
θ_{xu}=rotation angle of the upper end of column about the x axis
θ_y=slope of deflection curve of column about the y axis
θ_{yl}=rotation angle of the lower end of column about the y axis
θ_{y0}=deflection slope about the y axis at origin of the z axis (see Fig. 5)
θ_{yu}=rotation angle of the upper end of column about the y axis
σ=stress
σ_c=ultimate strength of concrete used in the analysis
σ_y=yield strength of reinforcing bar
ϕ_x=curvature about the x axis
ϕ_y=curvature about the y axis